Applied Mathematical Biosystems, Volume 1, Issue 1, (Jul-Dec 2025), 25-31

Applied Mathematical Biosystems

journal homepage: https://ambjournal.com

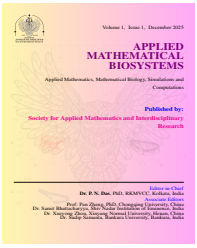

Comparative analysis of fractional-order and classical ODE models in explaining real-world dynamics

Phonindra Nath Das[1]

[1]*Department of Mathematics, Ramakrishna Mission Vivekananda Centenary College, Rahara, Kolkata-700118, West Bengal, India*

Abstract

Fractional calculus extends classical differential operators to non-integer orders, enabling the explicit modelling of memory and hereditary effects that are often absent in ordinary differential equation (ODE) formulations. This study evaluated fractional-order models formulated with the Caputo derivative against classical ODEs across four datasets: global population growth, enzyme kinetics, Indian rainfall, and blood glucose regulation. The parameters were estimated using least-squares optimisation, and the performance was evaluated based on the root mean square error (RMSE). In all cases, the fractional-order models achieved lower RMSE values, with improvements ranging from substantial to modest, yet systematic. Importantly, only one additional parameter, the fractional order (α), was introduced, preserving the model structure while enhancing accuracy. These results highlight fractional-order modelling as a flexible, interpretable, and computationally feasible framework for modelling complex dynamical systems.

Keywords: *Fractional differential equations; Caputo fractional derivative; Data-driven modeling; Memory effects; Root mean square error (RMSE)*

Corresponding author: Phonindra Nath Das *E-mail address:* pdas@rkmvccrahara.ac.in
Received: October 28th, 2025 **Revised:** December 21, 2025 **Accepted:** December 23, 2025 **Published:** December 26, 2025

1. Introduction

Fractional calculus has emerged as a rigorous mathematical framework that extends the concepts of classical differentiation and integration to arbitrary real or complex orders [1–3]. This generalization enhances the modeling capacity of differential equations by enabling system dynamics to be described not only through instantaneous rates of change but also through their historical evolution [3, 4]. Unlike local integer-order derivatives, fractional derivatives capture memory and hereditary effects [5]. Memory-dependent behavior is a defining feature of many natural systems, including hydrological processes, climate dynamics, and environmental series. In such contexts, the influence of past states persists across extended temporal scales, and conventional ordinary differential equation (ODE) models often fail to capture the full complexity of the observed data [6, 7]. Fractional differential equations (FDEs) provide an enriched modeling framework by introducing an additional degree of freedom, the fractional order α. This regulates the strength of the memory effects [4, 8]. This added flexibility frequently leads to improved model fit and enhanced predictive accuracy [6, 7]. The origins of fractional calculus can be traced back to a well-known correspondence dated 1695, in which L'Hopital asked Leibniz about the meaning of the derivative of non-integer order, specifically ($\alpha = \frac{1}{2}$). Leibniz suggested that this apparently paradoxical operator could produce meaningful results, a view now regarded as the conceptual origin of fractional calculus, not specifically fractional differentiation. Subsequent centuries saw significant efforts to rigorously formalize derivatives of arbitrary order. Notably, in 1730, Euler employed the identity

$$\frac{d^n(x^m)}{dx^n} = m(m-1)...(m-n+1)x^{m-n} = \frac{\Gamma(m+1)}{\Gamma(m-n+1)}x^{m-n}, \quad (1)$$

which expresses integer-order differentiation in terms of the gamma function. By extending this relation to non-integer values of n, Euler derived the following explicit formula for the half-order derivative:

$$\frac{d^{\frac{1}{2}}x}{dx^{\frac{1}{2}}} = \sqrt{\frac{4x}{\pi}}, \quad (2)$$

This result provided an early rigorous demonstration that fractional differentiation can be defined consistently via analytic continuation of classical operators. Building upon this foundational insight, experts have noted that the most influential formulation was later introduced by Riemann, who based his approach on Cauchy's integral formula.

$$\int_a^t ds_1 \int_a^{s_1} ds_2 ... \int_a^{s_{n-1}} y(s_n)ds_n = \frac{1}{(n-1)!}\int_a^t (t-s)^{n-1}y(s)ds, \quad (3)$$

Riemann introduced the concept of a fractional integral of order $\alpha > 0$ for a function $y : [a, b] \to \mathbb{R}$, defined as

$$ {}_aI_t^{\alpha} y(t) = \frac{1}{\Gamma(\alpha)} \int_a^t (t-s)^{\alpha-1} y(s) ds. \tag{4} $$

Building on this formulation, fractional derivatives are defined using a fractional integral operator. The Riemann-Liouville fractional derivative of order $\alpha > 0$ is expressed as

$$ {}_aD_t^{\alpha} y(t) = \left(\frac{d}{dt}\right)^n {}_aI_t^{n-\alpha} y(t) = \frac{1}{\Gamma(n-\alpha)} \left(\frac{d}{dt}\right)^n \int_a^t (t-s)^{n-\alpha-1} y(s) ds, \tag{5} $$

where $n \in \mathbb{N}$ is chosen such that $a \in (n-1, n)$. These definitions form the foundation of fractional operators, which until the 20th century were studied primarily within pure mathematics. Fractional calculus has become a significant tool across disciplines, including mathematics, mechanics [9], engineering [10], viscoelasticity [11], and dynamical systems [12]. By extending beyond integer-order derivatives, fractional operators enable more accurate modeling of real-world phenomena that exhibit memory and hereditary effects, such as viscoelasticity. Although the Riemann-Liouville derivative is historically important, it is often unsuitable for practical applications. Consequently, alternative formulations, such as the Caputo derivative, have been widely adopted owing to two key advantages: the derivative of a constant vanishes, and initial value problems depend only on integer-order derivatives. The Caputo fractional derivative of a function $y : [a, b] \to \mathbb{R}$ of order $\alpha > 0$ is defined as

$$ {}_a^C D_t^{\alpha} y(t) = {}_aI_t^{n-\alpha} y^n(t) = \frac{1}{\Gamma(n-\alpha)} \int_a^t (t-s)^{n-\alpha-1} y^n(s) ds, \tag{6} $$

where $n = [\alpha] + 1$. In the special case $\alpha \in (0, 1)$, this reduces to

$$ {}_a^C D_t^{\alpha} y(t) = \frac{1}{\Gamma(1-\alpha)} \int_a^t (t-s)^{-\alpha} y'(s) ds. \tag{7} $$

The fractional integral and fractional derivative act as inverse operators in the following sense ([2]):

Lemma 1.1 *Let $\alpha > 0$ and $n \in \mathbb{N}$ such that $\alpha \in (n-1, n)$. If $y \in AC^n[a, b]$, or $y \in C^n[a, b]$, then*

$$ {}_aI_t^{\alpha} \, {}_a^C D_t^{\alpha} y(t) = y(t) - \sum_{k=0}^{n-1} \frac{y^{(k)}(a)}{k!} (t-a)^k. \tag{8} $$

This result shows that the Caputo fractional derivative recovers the original function up to a polynomial correction, which is determined by the initial conditions. In particular, the correction term reflects the contribution of the lower-order derivatives at the initial point, thereby ensuring consistency with the classical differential operators.

Ordinary derivatives can be recovered as limiting cases of the Caputo fractional derivative when $\alpha \to n \in \mathbb{N}$. Specifically,

$$ \lim_{\alpha \to n^-} a^C D t^{\alpha} y(t) = y^{(n)}(t), \quad \lim_{\alpha \to n^+} a^C D t^{\alpha} y(t) = y^{(n)}(t) - y^{(n)}(a). $$

As an illustrative example, consider $y(t) = t^{1.5}$, $t \geq 0$. For $\alpha \in (0, 1)$, the Caputo derivative is

$$ {}_0^C D_t^{\alpha} y(t) = \frac{\Gamma(2.5)}{\Gamma(2.5-\alpha)} t^{1.5-\alpha}. \tag{9} $$

It follows that for $\alpha < 1.5$, we have $\frac{\Gamma(2.5)}{\Gamma(2.5-\alpha)} t^{1.5-\alpha}$ as an increasing function of t. In particular, for $\alpha = 1.5$ we have $\frac{\Gamma(2.5)}{\Gamma(1)} t^{1.5-1.5} \approx 1.32934$. As $\alpha > 1.5$, the derivative tends to zero. The behavior for different values of is illustrated in Figure 1. According to [13],

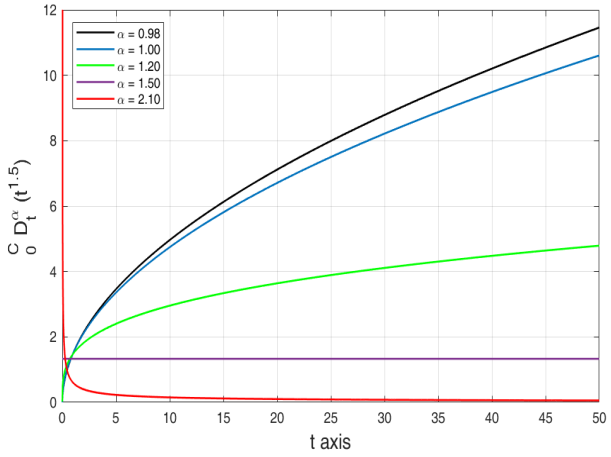

Figure 1. Caputo fractional derivatives of $y(t) = t^{1.5}$ for orders $\alpha \in 0.98, 1.0, 1.2, 1.5, 2.1$. Lower derivative orders yield smoother curves with reduced magnitudes, reflecting memory effects absent in the classical case $\alpha = 1$.

we have the following result

Theorem 1.2 *Suppose $f : [a, b] \times \mathbb{R} \to \mathbb{R}$ be continuous with $a < b$. For each $\alpha > 0$ let y_s be a solution on $[a, b]$ of the fractional initial-value problem*

$$ {}_a^C D_t^{\alpha} y_s(t) = f(t, y_s(t)), \qquad y_s(a) = y_a, $$

where ${}_a^C D_t^{\alpha}$ denotes the Caputo derivative of order α. Suppose the pointwise limit

$$ y^*(t) = \lim_{\alpha \to 1^{\pm}} y_s^*(t) $$

exists for every $t \in [a, b]$. Then y^* is a solution of the classical Cauchy problem

$$ y'(t) = f(t, y(t)), \qquad y(a) = y_a. $$

Proof: Consider $0 < \alpha < 1$, applying the Riemann–Liouville fractional integral operator ${}_aI_t^{\alpha}$ to the fractional equation and using the Lemma 1.1 yields the Volterra integral representation

$$ y_s(t) = y_a + \frac{1}{\Gamma(\alpha)} \int_a^t (t-z)^{\alpha-1} f(z, y_s(z)), dz, \qquad t \in [a, b]. \tag{10} $$

For fixed $t \in (a, b]$ define

$$ G_{\alpha}(t, z) = \frac{(t-z)^{\alpha-1}}{\Gamma(\alpha)} f(z, y_s(z)), \qquad z \in [a, t]. $$

By hypothesis $y_s(z) \to y^*(z)$ pointwise and continuity of f implies $f(z, y_s(z)) \to f(z, y^*(z))$ for each z. Moreover, for each fixed $z \in [a, t)$,

$$ \lim_{\alpha \to 1} \frac{(t-z)^{\alpha-1}}{\Gamma(\alpha)} = 1, $$

so $G_{\alpha}(t, z) \to f(z, y^*(z))$ pointwise on $[a, t]$ as $\alpha \to 1$. To pass the limit under the integral sign produces an integrable dominant. Since f is continuous on the compact set $[a, b] \times B$, where B is a

compact interval containing the values $y_s(z)$ for α near 1, there exists $M > 0$ such that $|f(z, y_s(z))| \le M$. The Gamma function is continuous at 1 and $\Gamma(1) = 1$, hence for α in a neighborhood of 1 we have $\Gamma(\alpha) \ge c > 0$. Consequently,

$$|G_\alpha(t,z)| \le \frac{M}{c}(t-z)^{\alpha-1} \le \frac{M}{c}(t-z)^{\delta-1}$$

for some fixed $\delta \in (0,1)$ and all $z \in [a,t]$. The function $(t-z)^{\delta-1}$ is integrable on $[a,t]$ since $\delta - 1 > -1$, so the Dominated Convergence Theorem applies. Thus

$$\lim_{\alpha\to 1} \frac{1}{\Gamma(\alpha)} \int_a^t (t-z)^{\alpha-1} f(z, y_s(z))dz = \int_a^t f(z, y^*(z))dz.$$

Passing to the limit in (10) yields the integral identity

$$[y^*(t) = y_a + \int_a^t f(z, y^*(z))dz \qquad \text{for all } t \in [a,b].$$

Differentiating with respect to t (the integrand is continuous) gives $y'(t) = f(t, y(t))$ on $(a,b]$, and evaluation at $t = a$ gives $y(a) = y_a$. Therefore, y^* solves the classical Cauchy problem, as claimed.

Note that the same argument adapts to limits $\alpha \to 1^+$ provided the extra initial derivatives appearing in the Lemma are controlled and converge; the core steps remain the Volterra representation and dominated convergence.

Parameter estimation for both the classical ordinary differential equation (ODE) model and the fractional-order model was performed using numerical optimization routines available in MATLAB. Specifically, the `lsqcurvefit` function was employed to calibrate each model against the experimental data by minimizing the least-squares error between the observed and simulated outputs. Model performance was assessed using the root-mean-square error (RMSE), defined for a dataset $\{y_i\}_{i=1\ldots m}$ with corresponding model predictions $\{u_i\}_{i=1\ldots m}$ as

$$\text{RMSE} = \sqrt{\frac{1}{m}\sum_{i=1}^{m}(y_i - u_i)^2}.$$

This metric provides a robust quantitative measure of the discrepancies between empirical observations and model predictions. Across all computational experiments, the fractional-order formulation consistently produced lower RMSE values than the classical ODE model, thereby demonstrating superior fidelity in capturing the underlying system dynamics.

In this study, we investigated four distinct real-world datasets, namely world population records, enzyme kinetics measurements, long-term Indian rainfall data, and clinical blood glucose observations, to assess the effectiveness of classical ODE models and their fractional generalizations formulated with the Caputo derivative. The aim was to determine whether incorporating fractional-order dynamics, and thereby introducing memory effects, leads to a more faithful representation of long-term variability, smoother trajectories, and reduced fitting error. For each dataset, we estimated the model parameters and the optimal fractional order α and evaluated the performance using the RMSE as a quantitative criterion. The overall objective is to identify when fractional models provide clear improvements over classical formulations and to highlight the versatility and robustness of fractional calculus in modeling complex biological, environmental, and population dynamics processes.

2. Population dynamics

2.1. ODE approach

There exist several attempts to describe the World Population Growth ([14]). The simplest model is the following, known as the Malthusian law of population growth, which is used to predict populations under ideal conditions. Let $N(t)$ be the number of individuals in a population at time t, B and M the birth and mortality rates, respectively, so that the net growth rate is given by

$$\frac{dN}{dt} = (B - M)N = rN, \tag{11}$$

where $r = B - M$ is the growth rate. Here, we assume that B and M are constant, and thus r is also constant. The solution of this differential equation is the function-

$$N(t) = N_0 e^{rt}, \ \ t \ge 0, \tag{12}$$

where N_0 is the population at $t = 0$. Because of the solution (12), this model is also known as the exponential growth model.

2.2. Fractional approach

Consider that the World Population Growth model is ruled by the fractional differential equation

$${}_0^C D_t^\alpha N(t) = rN(t), \ \ t \ge 0, \ \alpha \in (0,1). \tag{13}$$

Observe that, taking the limit $\alpha \to 1^-$, equation (13) converts into equation (11), but if we consider $\alpha \in (1,2)$ and take the limit $\alpha \to 1^+$, we obtain $N'(t) - N'(0) = rN(t)$.

Using the result by [15], the solution of this fractional differential equation is the function

$$N(t) = N_0 E_\alpha(rt^\alpha) \tag{14}$$

where $E_\alpha(\cdot)$ is the one parameter Mittag-Leffler function

$$E_\alpha = \sum_{k=0}^{\infty} \frac{t^k}{\Gamma(\alpha k + 1)}, \ \ t \in \mathbb{R}.$$

Consider now function (14), with $\alpha \in (0,2)$. Then, as $a \to 1^\pm$, we recover the solution for the classical problem (12).

2.3. Numerical simulation

For the numerical simulation, we employed population data provided by the United Nations Population Division (2013) [16], covering the period from 1910 to 2010 and consisting of 11 data points, with the initial value $N_0 = 1750$. The data were first plotted in a population-time framework. Subsequently, the classical ordinary differential equation (ODE) model approximation was superimposed on the same graph, followed by the fractional-order model approximation (see Figure 2). It is important to note that, in the case of the ODE model, the initial values were slightly adjusted to achieve a better fit; retaining the original initial condition resulted in an even poorer approximation. To quantitatively compare the predictive performance of the two models, the root mean square error (RMSE) was employed as an objective measure of goodness of fit. The classical ODE model yielded an RMSE of 171.13, whereas the fractional-order model achieved a markedly lower RMSE of 110.81. This substantial reduction in error indicates that the fractional-order model more accurately captures the underlying population dynamics and provides a superior fit to the observed data than the integer-order ODE model.

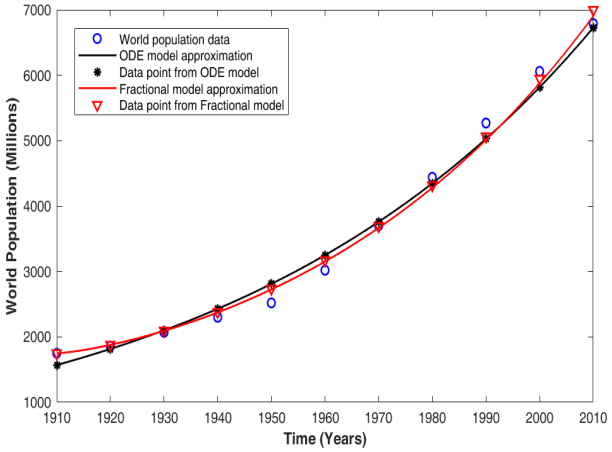

Figure 2. Population data from the United Nations (1910-2010) with model approximations. The plot compares the observed population values with the classical ordinary differential equation (ODE) model fit and the fractional-order model fit.

3. Enzyme kinetics dynamics

3.1. Classical saturation linear model

To describe the temporal evolution of the measured signal in the enzyme-reaction dataset reported in [17], we consider the classical saturation (or first-order relaxation) model

$$\frac{dS}{dt} = r\,(K - S(t)), \qquad t > 0, \tag{15}$$

where $S(t)$ denotes the observed reaction signal at time t, $r > 0$ is the kinetic relaxation rate, and $K > 0$ represents the asymptotic saturation level reached by the system. Such models arise naturally in biochemical kinetics when the observable quantity approaches a stable equilibrium value through a linear first-order process, typical of many enzyme-mediated reactions operating under quasi steady-state or pseudo first-order conditions. The dataset in [17], obtained for several acetoacetyl-CoA reductases, displays this characteristic saturation trend, making (15) a suitable descriptive model for fitting and parameter estimation.

Equation (15) is a linear first-order ordinary differential equation. Rewriting it in the standard form,

$$\frac{dS}{dt} + rS = rK,$$

and the explicit solution is

$$S(t) = K + (S_0 - K)\,e^{-rt}, \tag{16}$$

where, S_0 is the initial value of reaction substrate. This solution describes an exponential relaxation toward the saturation value K, with rate r, consistent with the behavior observed in the enzyme reaction data of [17].

3.2. Fractional approach of Saturation linear model

We consider the fractional extension of the classical saturation linear model. Its dynamics are described by the Caputo fractional differential equation given by

$${}_0^C D_t^{\alpha} S(t) = r\big(K - S(t)\big), \quad t \geq 0,\ \alpha \in (0,1), \tag{17}$$

This equation incorporates long-memory effects through the fractional order α. Now, the equation (17) can be rewritten as

$${}_0^C D_t^{\alpha} S(t) + rS(t) = rK. \tag{18}$$

The solution of the corresponding homogeneous equation is

$$S_c(t) = C\,E_{\alpha}(-rt^{\alpha}), \tag{19}$$

where $E_{\alpha}(\cdot)$ denotes the one-parameter Mittag–Leffler function $E_{\alpha}(z) = \sum_{k=0}^{\infty} \frac{z^k}{\Gamma(\alpha k+1)}$, $z \in \mathbb{R}$. Since the Caputo derivative of a constant is zero, the particular solution of (18) is

$$S_p(t) = K. \tag{20}$$

Thus, the general solution is

$$S(t) = K + C\,E_{\alpha}(-rt^{\alpha}). \tag{21}$$

Using the initial condition $S(0) = S_0$ and $E_{\alpha}(0) = 1$, we obtain $C = S_0 - K$. Therefore, the explicit solution of the fractional model (17) is

$$S(t) = K + (S_0 - K)\,E_{\alpha}(-rt^{\alpha}), \quad t \geq 0,\ \alpha \in (0,1). \tag{22}$$

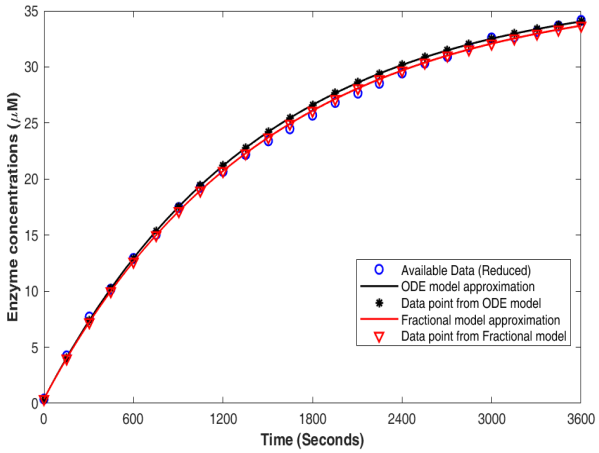

Figure 3. Comparison of experimental enzyme kinetics data with model approximations. The plot shows the original experimental observations, the classical ordinary differential equation (ODE) model fit, and the fractional-order ODE model fit. The fractional model demonstrates closer agreement with the experimental data than the classical ODE model.

3.3. Numerical simulation

The enzyme kinetics data set (*tspycdy2rm-1.zip*) was obtained from the experimental observations reported by [17]. Specifically, the data utilized in this study is located at the path: tspycdy2rm-1\AcAcCoA reductases data set\kinetic data\kinetic parameters estimations\AARChimera3\NADH.

The raw data were converted into Excel format for further processing. Among the 24 available data sets, curve13 was selected and reduced from 451 observations to 25, while preserving the overall kinetic pattern. To analyze the data, we employed both a classical ordinary differential equation (ODE) model and its fractional-order counterpart. The experimental data, together with the ODE and fractional approximations, are presented in Figure 3.

For quantitative comparison, the Root Mean Square Error

(RMSE) was calculated for both models. The ODE model yielded an RMSE of 0.523334, whereas the fractional model achieved a lower RMSE of 0.300257. These results demonstrate that the fractional-order model provides a superior fit to the experimental data compared to the classical ODE approach.

4. Average rainfall in India

Long-term rainfall variability plays a crucial role in hydrological forecasting, climate analyses, and agricultural planning. To investigate the temporal evolution of average Indian rainfall between 1901 and 2014, data were collected from the website of [18]. We considered a data-driven differential equation model. The observed rainfall pattern displays pronounced nonlinear temporal variability, thereby motivating the incorporation of polynomial forcing terms within both ordinary differential equations and their fractional counterparts.

4.1. Modelling approach

We consider the first-order ODE

$$\frac{dW}{dt} = a_1 t^4 + a_2 t^3 + a_3 t^2 + a_4 t + a_5, \tag{23}$$

where $W(t)$ denotes rainfall intensity and $a_1, \dots, a_5$ are model parameters. Integrating both sides of equation (23) yields

$$W(t) = \frac{a_1}{5} t^5 + \frac{a_2}{4} t^4 + \frac{a_3}{3} t^3 + \frac{a_4}{2} t^2 + a_5 t + C, \tag{24}$$

where C is determined using the initial rainfall value $W(0)$.

The solution takes the form of a fifth-degree polynomial, allowing the capture of complex nonlinear rainfall dynamics. The model remains deterministic and smooth, offering a stable analytical framework for long-term prediction. While higher-order polynomial forcing enhances flexibility, it may also amplify sensitivity to noise; hence, a balance between interpretability and smoothness is essential.

4.2. Fractional Differential Model

To incorporate memory and hereditary effects inherent in climatic systems, we generalize equation (23) using the Caputo fractional derivative:

$${}_0^C D_t^\alpha W(t) = a_1 t^4 + a_2 t^3 + a_3 t^2 + a_4 t + a_5, \qquad 0 < \alpha \le 1. \tag{25}$$

The solution of equation (25) is obtained by applying fractional integration:

$$W(t) = W(0) + \sum_{i=1}^{5} \frac{a_i}{\Gamma(\alpha + 6 - i)} t^{\alpha+5-i}. \tag{26}$$

Fractional models incorporate memory effects, enabling long-term rainfall influences to persist across temporal scales. When the formulation reduces to the classical ODE model, it ensures consistency. Since the forcing is polynomial, the Mittag-Leffler family is unnecessary, and fractional integration remains algebraic. The fractional-order parameter governs smoothness and historical dependence, thereby enhancing flexibility in the representation of climatic datasets.

4.3. Numerical simulation

Parameter estimation was performed by calibrating the model outputs against the observed monthly rainfall time series. For the ordinary differential equation (ODE) model (23), a least-squares optimization was applied to the polynomial solution, resulting in the parameter set $(a_1, a_2, a_3, a_4, a_5, a_6) = (0.0767, -2.5222, 30.4054, -156.0503, 263.9710, 147.8883)$, which yielded the closest correspondence with the long-term mean rainfall data. In the fractional-order formulation, the same parameter set was retained, while the fractional order α was treated as the free variable. The optimal fit occurs at $\alpha = 0.985$, indicating that the inclusion of a mild memory effect improves the model's descriptive power. Comparative plots of both model approximations alongside the empirical data are presented in Figure 4.

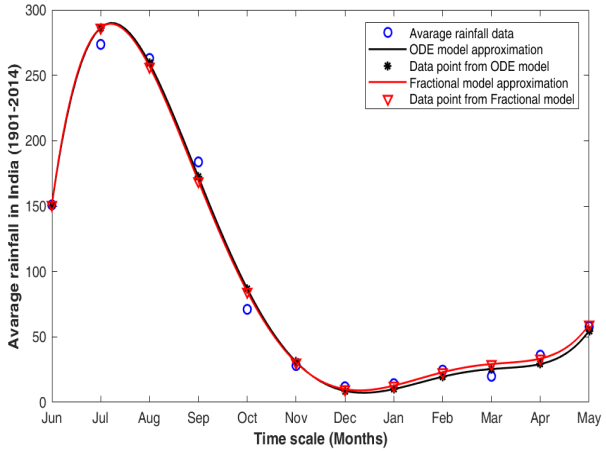

Figure 4. Two dimensional parameter space anaysis with e versus other sensitive parameters. The system shows oscillation in the red colored regions and in green colored region system does not show any oscillations.

The accuracy of the fits was evaluated using the root-mean-square error (RMSE). The ODE model produced an RMSE of 7.6855, whereas the fractional model achieved a slightly lower RMSE of 7.6036. Although the reduction in error is modest, the fractional model exhibits a marginally improved performance, consistent with the enhanced visual agreement observed in Figure 4.

5. Blood glucose levels

5.1. ODE approach

Following [19], we obtain a simple model to determine the Blood glucose level, described by a two-dimensional system of ordinary differential equations. Let S be the concentration of glucose generated due to the consumption of food, and G be the concentration of glucose in the blood. Then the problem can be described by the following Cauchy system:

$$\begin{aligned} \frac{dS}{dt} &= -pS, \\ \frac{dG}{dt} &= c + pS - qG, \end{aligned} \tag{27}$$

where, $S(0) = S_0$ is the initial amount of glucose, $G(0) = G_0$ is the initial amount of blood glucose level. The constant denotes the glucose input rate from cellular storage, while and are positive constants representing, respectively, the glucose release rate from food sources and the blood glucose degradation rate. Now the solution of (27) is given by the following two functions

$$S(t) = S_0 e^{-pt}, \tag{28}$$

and

$$G(t) = S_0 \frac{p}{q-p} e^{-pt} + \left(G_0 - S_0 \frac{p}{q-p} - cq \right) e^{-qt} + cq. \quad (29)$$

From [19], a set of experimental data is obtained in order to determine the arbitrary constants p and q, where time is in minutes and the blood glucose level (BGL) in mg/dL.

5.2. Fractional approach

Now we show that, if we consider the problem modeled by a system of fractional differential equations, we obtain a curve that better fits the experimental results. Let $\alpha, \beta \in (0,1)$ and consider the system of fractional differential equations

$$\begin{aligned} {}_0^C D_t^\alpha S(t) &= -pS, \\ {}_0^C D_t^\beta G(t) &= c + pS - qG. \end{aligned} \quad (30)$$

Following Diethelm (2010) [15], the solution with respect to S is

$$S(t) = S_0 E_\alpha(-pt^\alpha). \quad (31)$$

To determine G, it can be found as the solution of a fractional differential linear equation

$${}_0^C D_t^\beta G(t) = c - qG(t) + pS_0 E_\alpha(-pt^\alpha). \quad (32)$$

Similarly, we obtain the solution with respect to G, as $G(t)$

$$\begin{aligned} &= G_0 E_\beta(-qt^\beta) + \beta \int_0^t \left\{ pS_0 E_\alpha(-p(t-s)^\alpha) + c \right\} s^{\beta-1} E'_\beta(-qs^\beta) ds \\ &= p\beta S_0 \int_0^t \sum_{m=0}^\infty \frac{(-p)^m (t-s)^{m\alpha}}{\Gamma(m\alpha+1)} s^{\beta-1} \sum_{n=0}^\infty \frac{(n+1)(-q)^n s^{n\beta}}{\Gamma(n\beta+\beta+1)} ds \\ &\quad + c\beta \int_0^t \sum_{n=0}^\infty \frac{(n+1)(-q)^n s^{n\beta}}{\Gamma(n\beta+\beta+1)} s^{\beta-1} ds + G_0 \sum_{k=0}^\infty \frac{(-q)^k t^{k\beta}}{\Gamma(k\beta+1)} \\ &= p\beta S_0 \sum_{m=0}^\infty \sum_{n=0}^\infty \frac{(n+1)(-p)^m (-q)^n}{\Gamma(m\alpha+1)\Gamma(n\beta+\beta+1)} \int_0^t (t-s)^{m\alpha} s^{n\beta+\beta-1} ds \\ &\quad + c\beta \sum_{n=0}^\infty \frac{(n+1)(-q)^n}{\Gamma(n\beta+\beta+1)} \int_0^t s^{n\beta+\beta-1} ds + G_0 \sum_{k=0}^\infty \frac{(-q)^k t^{k\beta}}{\Gamma(k\beta+1)} \\ &= p\beta S_0 \sum_{m=0}^\infty \sum_{n=0}^\infty \frac{(n+1)(-p)^m (-q)^n}{\Gamma(m\alpha+1)\Gamma(n\beta+\beta+1)} \int_0^t (t-s)^{m\alpha} s^{n\beta+\beta-1} ds \\ &\quad + c \sum_{n=0}^\infty \frac{(-q)^n}{\Gamma(n\beta+\beta+1)} t^{n\beta+\beta} + G_0 \sum_{k=0}^\infty \frac{(-q)^k}{\Gamma(k\beta+1)} t^{k\beta}. \end{aligned} \quad (33)$$

We remark that, as the expression inside the series is continuous and uniformly convergent, the previous calculations are valid. Let us re-write function B(·) using the Beta function, as follows

$$\mathrm{B}(a,b) = \int_0^1 t^{a-1}(1-t)^{b-1} dt, \quad \text{where} a, b > 0, \quad (34)$$

with the following property

$$\mathrm{B}(a,b) = \frac{\Gamma(a)\Gamma(b)}{\Gamma(a+b)},$$

and doing the change of variables $u = \frac{s}{t}$, we obtain

$$\begin{aligned} \int_0^t (t-s)^{m\alpha} s^{n\beta+\beta-1} ds &= t^{m\alpha+n\beta+\beta} \int_0^t (1-u)^{m\alpha} u^{n\beta+\beta-1} du \\ &= t^{m\alpha+n\beta+\beta} \mathrm{B}(n\beta+\beta, m\alpha+1) \\ &= t^{m\alpha+n\beta+\beta} \frac{\Gamma(n\beta+\beta)\Gamma(m\alpha+1)}{\Gamma(n\beta+\beta+m\alpha+1)}. \end{aligned} \quad (35)$$

Hence, using (35) into (33) we obtain

$$\begin{aligned} G(t) &= G_0 \sum_{k=0}^\infty \frac{(-q)^k}{\Gamma(k\beta+1)} t^{k\beta} + c \sum_{n=0}^\infty \frac{(-q)^n}{\Gamma(n\beta+\beta+1)} t^{n\beta+\beta} \\ &\quad + pS_0 \sum_{m=0}^\infty \sum_{n=0}^\infty \frac{(-k_1)^m (-k_2)^n}{\Gamma(n\beta+\beta+m\alpha+1)} t^{m\alpha+n\beta+\beta}. \end{aligned} \quad (36)$$

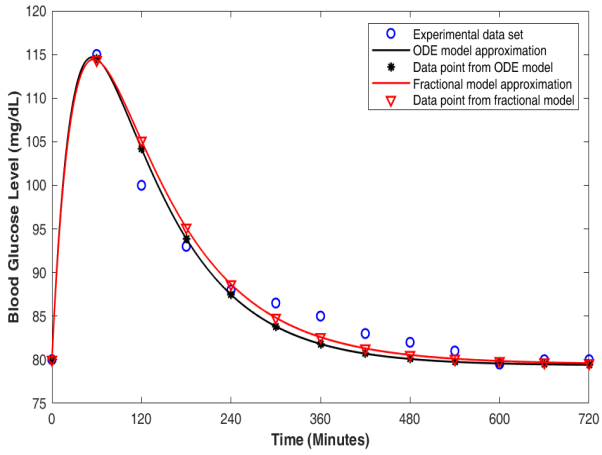

Figure 5. Comparison of experimental blood glucose data reported by [19] with model simulations. The figure illustrates the measured glucose concentrations alongside the fitted classical ODE solution and the fractional-order model solution ($\alpha = 0.99$), both obtained using the same parameter set.

5.3. Numerical simulation

Using the experimental blood glucose dataset reported by [19], model parameters were estimated by minimizing the mean absolute error between measured glucose concentrations and simulated outputs. For the classical ordinary differential equation (ODE) formulation, the optimal parameter set was identified as $p = 0.01$, $q = 0.0305$, and $c = 2.42$. The resulting ODE-based glucose trajectory is presented in Figure 5 alongside the experimental observations.

Subsequently, these parameter values were applied to the fractional-order formulation of the model, with the fractional derivative order fixed at $\alpha = 0.99$. The numerical solution of the fractional-order system was computed and superimposed on the same figure, enabling direct comparison with both the experimental data and the classical ODE approximation.

To quantitatively evaluate model performance, the root mean square error (RMSE) was calculated using the experimental data as reference. The classical ODE model yielded an RMSE of 1.9145 mg/dL, whereas the fractional-order model achieved a slightly lower RMSE of 1.8912 mg/dL. Although the improvement is modest, the consistent reduction in error demonstrates that the fractional-order formulation provides a more accurate representation of glucose dynamics compared to the integer-order ODE model.

6. Conclusions

In this study, we conducted a comparative analysis of classical integer-order ordinary differential equation (ODE) models and their fractional-order counterparts. We examined diverse real-world case studies, including global population growth,

enzyme kinetics, rainfall dynamics, and blood glucose regulation. These examples span multiple domains and data characteristics, providing a robust framework for assessing the benefits of fractional-order modeling.

Across all cases, fractional-order models consistently achieved lower root mean square error (RMSE) values than classical ODE formulations. In population dynamics, the fractional model substantially improved the fit to United Nations data, reflecting its ability to capture long-term memory effects inherent in demographic evolution. For enzyme kinetics, the fractional approach yielded markedly superior agreement, highlighting the role of memory-dependent dynamics in biochemical processes. In rainfall modeling, although the reduction in RMSE was modest, the fractional formulation yielded improved descriptive accuracy, indicating that even weak memory effects can enhance the representation of climatological time series. A comparable trend emerged in blood glucose regulation, where the fractional-order model consistently achieved lower RMSE under identical parameter sets.

Importantly, the fractional formulation required only one additional parameter-the fractional order (α)-while preserving the structural form and parameterization of the classical models. This minimal increase in complexity produced measurable gains in accuracy and improved qualitative agreement with experimental data.

Overall, the findings indicate that fractional-order models constitute a natural extension of classical ODEs, seamlessly incorporating memory and hereditary effects. They offer a flexible and interpretable framework for analyzing dynamical systems, while remaining computationally efficient and delivering improved predictive performance.

7. Acknowledgements

The author gratefully acknowledges the learned reviewer for their insightful comments and valuable suggestions. The constructive feedback provided during the review process has been instrumental in enhancing the rigor, clarity, and overall quality of this article. The author sincerely appreciates the reviewer's time and expertise, which significantly contributed to the refinement of the manuscript.

REFERENCES

[1] I. Podlubny. *Fractional Differential Equations*, volume 198 of *Mathematics in Science and Engineering*. Academic Press, San Diego, CA, 1999.

[2] A. A. Kilbas, H. M. Srivastava, and J. J. Trujillo. *Theory and Applications of Fractional Differential Equations*, volume 204 of *North-Holland Mathematics Studies*. Elsevier Science B.V., Amsterdam, 2006.

[3] N. Su. *Fractional Calculus for Hydrology, Soil Science and Geomechanics: An Introduction to Applications*. CRC Press, 1 edition, 2020. .

[4] R. A. Patil and S. A. Sayed. A Comprehensive Review of Fractional Differential Equations and Their Role in Modeling Complex Dynamical Systems. *International Journal of Engineering, Science and Humanities*, 14(4):71–80, 2024.

[5] S. Pramanik, K. P. Das, P. Karmakar, and S. Sarkar Mondal. A Comprehensive Review on Fractional Models Involving Ecology and Eco-epidemiology. *Journal of Applied Math*, 1 (4):236, 2023.

[6] M. Borthwick. *Application of Fractional Calculus to Rainfall Streamflow Modelling*. PhD thesis, University of Plymouth, 2010. PhD Thesis, deposited 2024.

[7] Y. J. Yoon and J. C. Kim. Fractional Linear Reservoir Model as Elementary Hydrologic Response Function. *Water*, 15 (24):4254, 2023.

[8] P. Roy. The Rise of Fractional Calculus: Novel Applications in Engineering and Biological Systems. *Recent Trends in Mathematics*, 01(02):7–11, 2025.

[9] T. M. Atanackovic, S. Pilipovic, B. Stankovic, and D. Zorica. *Fractional Calculus with Applications in Mechanics: Vibrations and Diffusion Processes*. Wiley–ISTE, 2014.

[10] J. A. T. Machado, M. F. Silva, R. S. Barbosa, I. S. Jesus, C. M. Reis, M. G. Marcos, and A. F. Galhano. Some Applications of Fractional Calculus in Engineering. *Mathematical Problems in Engineering*, 2010:Article ID 639801, 2010. 34 pages.

[11] F. C. Meral, T. J. Royston, and R. Magin. Fractional Calculus in Viscoelasticity: An Experimental Study. *Communications in Nonlinear Science and Numerical Simulation*, 15(4):939–945, 2010.

[12] V. E. Tarasov. *Applications of Fractional Calculus to Dynamics of Particles, Fields and Media*. Nonlinear Physical Science. Springer, 2010.

[13] R. Almeida, N. R. Bastos, and M. T. T. Monteiro. Modeling Some Real Phenomena by Fractional Differential Equations. *Mathematical Methods in the Applied Sciences*, 39(16):4846–4855, 2016.

[14] D. A. Smith. Human Population Growth: Stability or Explosion? *Mathematics Magazine*, 50(4):186–197, 1977.

[15] K. Diethelm. *The Analysis of Fractional Differential Equations: An Application-Oriented Exposition Using Differential Operators of Caputo Type*, volume 2004 of *Lecture Notes in Mathematics*. Springer, 2010.

[16] United Nations. World population prospects: the 2012 revision. Volume 2: demographic profiles, UN. Population Division, UN, 2013.

[17] K. Olavarria. Kinetic Data from Different Acetoacetyl-CoA Reductases, 2021. Technische Universiteit Delft, Version 1.

[18] Government of India. All India Area Weighted Monthly, Seasonal and Annual Rainfall (1901–2014), 2014. URL https://mausam.imd.gov.in/.

[19] G. Freckmann, S. Hagenlocher, A. Baumstark, N. Jendrike, R. C. Gillen, K. Rössner, and C. Haug. Continuous Glucose Profiles in Healthy Subjects under Everyday Life Conditions and after Different Meals. *Journal of Diabetes Science and Technology*, 1(5):695–703, 2007.